
NO SHIFTED AUGMENTATIONS (NSA): COMPACT DISTRIBUTIONS FOR ROBUST SELF-SUPERVISED ANOMALY DETECTION

Mohamed Yousef¹, Marcel Ackermann¹, Unmesh Kurup^{1*}; Tom Bishop^{2*}

¹Intuition Machines, Inc.

²Glass Imaging, Inc. ‡

{myb,marcel,unmk}@imachines.com,tom@glass-imaging.com

ABSTRACT

Unsupervised Anomaly detection (AD) requires building a notion of normalcy, distinguishing in-distribution (ID) and out-of-distribution (OOD) data, using only available ID samples. Recently, large gains were made on this task for the domain of natural images using self-supervised contrastive feature learning as a first step followed by kNN or traditional one-class classifiers for feature scoring. Learned representations that are non-uniformly distributed on the unit hypersphere have been shown to be beneficial for this task. We go a step further and investigate how the *geometrical compactness* of the ID feature distribution makes isolating and detecting outliers easier, especially in the realistic situation when ID training data is polluted (i.e. ID data contains some OOD data that is used for learning the feature extractor parameters). We propose novel architectural modifications to the self-supervised feature learning step, that enable such compact distributions for ID data to be learned. We show that the proposed modifications can be effectively applied to most existing self-supervised objectives, with large gains in performance. Furthermore, this improved OOD performance is obtained without resorting to tricks such as using strongly augmented ID images (e.g. by 90 degree rotations) as proxies for the unseen OOD data, as these impose overly prescriptive assumptions about ID data and its invariances. We perform extensive studies on benchmark datasets for one-class OOD detection and show state-of-the-art performance in the presence of pollution in the ID data, and comparable performance otherwise. We also propose and extensively evaluate a novel feature scoring technique based on the angular Mahalanobis distance, and propose a simple and novel technique for feature ensembling during evaluation that enables a big boost in performance at nearly zero run-time cost compared to the standard use of model ensembling or test time augmentations. Code for all models and experiments will be made open-source.

1 INTRODUCTION

Anomaly detection (AD) or out-of-distribution (OOD) detection requires using only available in-distribution (ID) samples for training a classifier to decide upon the relative normalcy of samples at test time, without knowledge of the nature of the OOD data. OOD detection is an important problem with practical applications in, for example, industrial defect detection, fraud detection, autonomous driving, biometrics, spoofing detection and many other domains (Tack et al., 2020).

1.1 BACKGROUND

For natural images (which according to the manifold hypothesis lie in a compact set in a suitable space), OOD detection translates to finding as tight a decision boundary as possible around the normal set, while excluding unseen samples from other classes or distributions. This detection was

*Equally contributing last authors.

‡Work done while at Intuition Machines, Inc.

traditionally done with either generative (Zhai et al., 2016) or discriminative models (Schölkopf et al., 2000) on top of shallow features. Deep representations subsequently provided a large boost in performance. However, the density of deep generative image models have often proved to be ineffective (Kingma & Dhariwal, 2018), with poorly calibrated likelihoods away from observed data. There have instead been two recent directions to learn suitable deep features used for OOD evaluation: a) supervised pre-training on an external dataset. b) Self-supervised learning (SSL) pre-training on either the normal set only or also on an external dataset. A variety of learned metrics, scoring functions, or one-class classifiers have then been employed on top of these learned features and this general paradigm has shown to be highly effective in many cases (Sohn et al., 2020).

The best recent results with SSL-based training for OOD has been with contrastive learning (Tack et al., 2020; Sohn et al., 2020; Sehwan et al., 2021; Winkens et al., 2020). Contrastive learning has been shown to distribute ID data uniformly on the hypersphere (Wang & Isola, 2020). While this helps general multi-class SSL training, it hurts OOD detection, as it makes isolating outliers from the single class harder (Sohn et al., 2020). This uniformity also makes OOD detection much more sensitive to pollution in the inlier training data (Han et al., 2021; Sohn et al., 2020). See Appendix H for more background on related methods.

If some labeled OOD data are available as negatives, semi-supervised learning maybe be used (Ruff et al., 2018; Han et al., 2021). If no such labeled negatives are available, one way to soften the effect of a contrastively learned uniform representation is to introduce artificial negative samples as proxies for these outliers. Using hard augmentations (e.g. 90 degree rotations) has been termed *Distributional Shifting* (Tack et al., 2020; Sohn et al., 2020; Li et al., 2021; Tian et al., 2021). Such augmentations are intended to make the in-distribution data less uniform, and thus easier to isolate from OOD data. However, they also make the significant assumption that the data is not (fully or partially) invariant to those augmentation(s), and that the augmentations are a good proxy for the true negative distribution.

The other direction is using features from a model pre-trained on a large external dataset, with the hope of producing universal features that can work in any OOD detection scenario. This can be done in either supervised (Reiss et al., 2020) or self-supervised manner (Xiao et al., 2021). However, the assumption that such representative labeled samples will be available in the latter case, or that learned image features from general datasets such as ImageNet will transfer well may be restrictive at best.

1.2 CONTRIBUTION

In this work, we first investigate the training dynamics of contrastive SSL methods, and show that their performance decays significantly over long term training. We find that uniformity or non-compactness of the learned ID representation is the main reason for this decay. We study this effect on positive-pairs-only SSL using SimSiam (Chen & He, 2020), and show that in such cases, the decay does not happen.

We propose an architectural modification that can be applied generally across such networks, and show extensive analysis that this modification improves performance and always encourages learning a more compact ID representations. In doing so we are able to learn high quality One-class classifiers without resorting to distributionally shifted augmented samples as negatives, hence we term the resulting methodology *No Shifted Augmentations* (NSA). We summarize our contributions as follows:

- We investigate and empirically verify and quantify that the non-uniformity and compactness of learned ID is a main factor of the final OOD detection performance, independent from the quality of the learned features.
- We propose an assumption-free, simple and novel architectural modification for inducing a non-uniform learned ID representation, and show that this works very well with both SimSiam and SimCLR and produces solid performance improvements.
- We identify, investigate, and solve a gradient problem in SimSiam (and also BYOL) that greatly affects the proper propagation of the norms inside the network; we solve it and notice much higher stability, especially in the low batch size training regime.
- We consider improved feature scoring methods for OOD detection, including in our proposed solution a Mahalanobis Cosine score on nearest neighbors, related to methods in open-set metric learning. We then present a computationally efficient method of feature ensembling that also boosts performance.

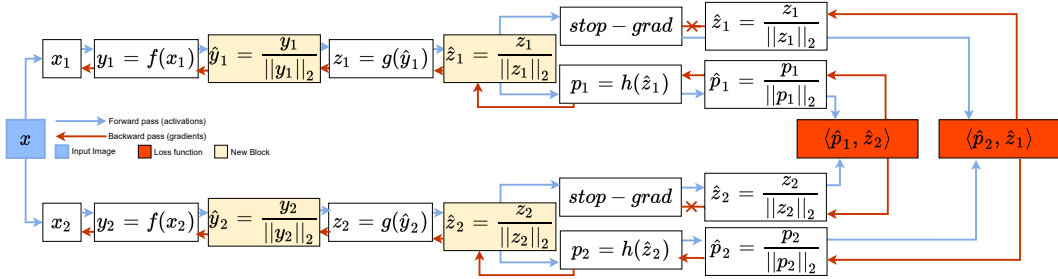


Figure 1: An illustration of modified SimSiam with the yellow boxes showing our proposed changes described in Sec. 2.3, 2.4. In the original version the gradients of $\hat{z}_i = z_i / \|z_i\|_2$ are prevented from flowing backwards in *all possible paths* by the stop-grad operation. In our modified version, thanks to the added operations, we can mimic the flow of the gradients of $\hat{z}_i = z_i / \|z_i\|_2$ that were blocked.

- We show unexpected case(s) (e.g. SVHN) where the usual ImageNet-Pretrained ResNet methods fail catastrophically on One-Class Classification Anomaly Detection tasks, even with feature adaptation. We show that training from scratch without using shifted augmentations avoids this.
- We extensively evaluate and ablate the proposed models with a wide variety of different datasets and scenarios, separating the contributions of representation learning, scoring, data augmentation, and additional variations like ensembling. We show our solutions have comparable performance against more complex methods. More importantly they show state-of-the-art performance, by a wide margin, achieving robustness for small batch sizes and in the presence of polluted data.

2 METHODOLOGY

2.1 SELF-SUPERVISED LEARNING (SSL) SETUP

A general SSL setup resembling SimSiam (Chen & He, 2020) is depicted in Figure 1. SimCLR is a very similar architecture that omits a prediction network, so we use SimSiam for this illustration. The figure shows both the forward pass and backward pass of two random augmentations x_1 and x_2 of an input image x . Both are encoded by the shared encoder (the convolutional backbone network) f into y_1 and y_2 . Both augmentations are projected into z_1 and z_2 by a projection network g . A prediction network h transforms z_i into $p_i = h(z_i)$ and the whole network learns to match the output of the prediction network fed with the projection of one view $p_i = h(z_i)$ to the projection of the other view $z_j = g(y_j)$ and vice versa, by minimizing their negative cosine similarity:

$$\mathcal{D}(p_i, z_j) = -\frac{p_i}{\|p_i\|_2} \cdot \frac{z_j}{\|z_j\|_2}. \quad (1)$$

Most current SSL algorithms use a projection head g on top of a convolutional feature extractor, as this was empirically found to help learn a much better final representation (Chen et al., 2020a;b; Grill et al., 2020b; Chen & He, 2020). However, it was also found that the learned projection is much worse in downstream tasks (Chen et al., 2020a) including for OOD (Sohn et al., 2020). Therefore, the output of the encoder backbone f used during feature evaluation in most OOD methods is based on SSL, as it learns a much better representation. We call the outputs of f the learned embedding.

2.2 IS REPRESENTATION QUALITY THE ONLY IMPORTANT THING FOR OOD ?

To illustrate that the quality of learned representation is only one factor for OOD performance, we train SimCLR on one class of CIFAR10 and evaluate the learned representation for OOD detection against all other classes; a similar setup is used in (Sehwag et al., 2021; Tack et al., 2020), however, we train for much longer. We repeat this experiment for 4 different classes, and evaluate the learned representations for OOD detection for each throughout training. Figure 2a (blue curve) shows the mean performance evaluation of the 4 classes; it is evident that performance reaches a peak very fast

(within few hundred epochs) then deteriorates significantly as training progresses. Appendix A shows the same phenomena using 2 other evaluation metrics, with detailed graphs for each class.

One easy way to explain this behavior is the deteriorating quality of the learned representation. We carry out two more evaluations to examine this hypothesis. In Figure 2c we use linear evaluation (Zhang et al., 2016) and weighed k-NN (Wu et al., 2018) to evaluate the quality of learned representation. Figure 3d shows that the quality of the representation barely changes during training, i.e. there is only the expected small decrease after the peak and then just fluctuations, and that linear separability holds. Weighted k-NN results supporting the same fact are in Appendix A.

These results tell two stories. (a) Methods based on density estimation show that performance drops down significantly as training progresses. (b) Doing supervised classification on the frozen features shows they are still of high quality and maintain nearly the same linear separable performance of the learned representation. This points to a change of the underlying distribution of the embedding space.

To study what is happening, we use the von Mises-Fisher (vMF) distribution which is a fundamental probability distribution on the $(n - 1)$ -dimensional hyper-sphere $S^{d-1} \subset R^d$. Its probability density function is $f_n(z, \mu, \kappa) = C_n(\kappa)e^{\kappa\mu^T z}$, where μ is the mean direction, and κ is the concentration parameter. The vMF shape depends on κ : for high values, the distribution has a mode at the mean direction μ ; for $\kappa = 0$ it is uniform on the hyper-sphere S^{d-1} . vMF has been successfully used in both analyzing (Wang & Isola, 2020; Lee et al., 2018a; 2021) and learning (Hasnat et al., 2017; Davidson et al., 2018; Kumar & Tsvetkov, 2018) deep neural networks.

We fit a vMF (Banerjee et al., 2005; Sra, 2012) to the learned normalized embeddings of SimCLR, and study how κ changes during training. Figure 2b shows how SimCLR starts with a relatively large κ (high concentration) then reduces monotonically (low concentration, more uniform) as training progresses – this is true for both ID and OOD. In Figure 2f we notice the same behaviour using another tool: the Maximum Mean Discrepancy (MMD) (Gretton et al., 2012) between the learned representation and samples from a uniform distribution on a unit hypersphere, as suggested in (Sohn et al., 2020). MMD measures the distance between two probability distributions, so a high MMD means a less uniform and more concentrated distribution, and a low MMD the opposite.

Observe that this gives an explanation of the decaying performance seen in Figure 2a (blue curve). It is not the quality of the representation that is essential, but rather its distribution. As the ID data distribution gets more uniform, the probability p to find an inlier sample $x \in \text{ID}$ arbitrarily close to an outlier query sample $x' \in \text{OOD}$ increases, i.e. ID and OOD get more and more indistinguishable. This is exactly the intuition behind many methods for AD, for example (Ruff et al., 2018; Goyal et al., 2020; Ruff et al., 2021)

Given this analysis, and the fact that contrastive methods are proven to converge to a uniform distribution (Wang & Isola, 2020), we take the natural step and perform the same analysis on a non-contrastive SSL method, SimSiam (selected over BYOL as it is simpler and retains most of the performance). Results are shown in Figure 2c, 2d, where indeed there is big difference from SimCLR: OOD performance stays nearly constant after reaching the peak. Also in Figure 2e, 2f we see that although the representation is also becoming more uniform, it is at a much slower rate, and is able to maintain high values for κ and MMD even after many epochs of training.

It is also important to mention that this analysis shows that the number of training epochs (or use of early stopping criteria) is a very important hyper-parameter to choose for contrastive methods used for OOD. This needs to be carefully tuned, and we see that non-contrastive methods have a big advantage in being less sensitive to the number of epochs. Other works that noticed importance of early stopping in this context include (Reiss et al., 2020; Han et al., 2021; Reiss & Hoshen, 2021)

2.3 LEARNING A DENSE REPRESENTATION

(Schmidt et al., 2018) show that the sample complexity of robust learning can be significantly larger than that of standard learning. While some works tried to address this difference with extra positive or negative data, (Pang et al., 2019) propose the interesting idea of manipulating the local sample distribution of the training data via appropriate training objectives such that by inducing high-density feature regions, there would be locally sufficient samples to train robust classifiers and return reliable predictions. We propose pursuing the same direction with the OOD detection problem, and propose an architectural modification that can help induce high density feature space.

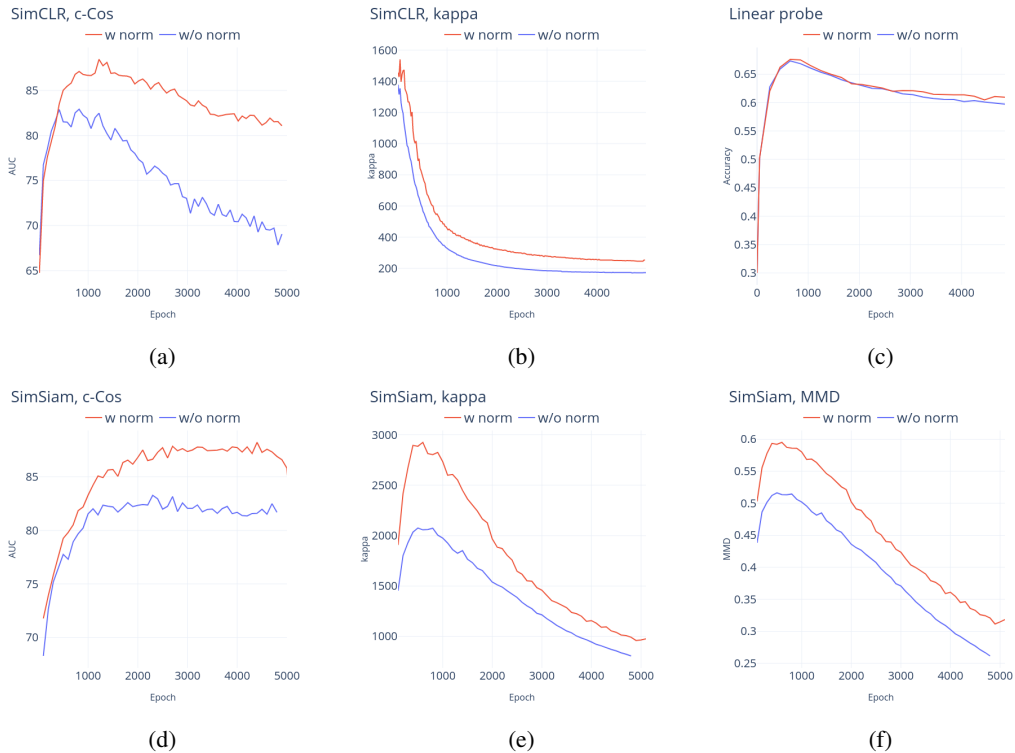


Figure 2: Analysis of training and evaluation of SimCLR and SimSiam on CIFAR10 for OOD with and without the proposed normalization. Every point on these plots represents the average from 4 independent classes. First row, SimCLR evaluated with (a) $c\text{-Cos}$ (b) κ from fitting a vMF (c) linear probe accuracy. Second row, SimSiam evaluated with (d) $c\text{-Cos}$ (e) κ from fitting a vMF (f) Maximum Mean Discrepancy (MMD) with a uniform distribution.

We propose adding a differentiable l_2 -normalization operation after the encoder f and before the projection head g . As such, the output $y_i = f(x_i)$ is transformed into $\hat{y}_i = y_i / \|y_i\|_2$ (as in Figure 1). The intuition is that adding the normalization step would deprive the model of any gradients when the norm of the embedding is changed, thus enforcing the model to learn directional transformations as those would be the only way to actually decrease the loss function. Regularizing the model this way should give a finer directional control on the learned embedding (the cosine distance makes more sense), and yield a more efficient use of volume and thus a denser representation.

We perform a series of experiments to empirically verify our intuition. Figure 2a (red curve) shows evaluation logs for SimCLR after adding normalization. It is evident the training is much more regularized now, the decrease in OOD performance after the peak is much smaller and performance is maintained for thousands of epochs. Figure 2b (red curve) shows a denser learned representation when compared to original SimCLR. We can see the same behaviour for SimSiam in Figure 2d, 2e.

One thing to note here that greatly strengthens the analysis made in the previous section, is the linear probe accuracy with and w/o norm (Figure 2c), they are essentially the same, even after 5000 epochs, on the other hand there is big difference between their OOD performance at that point (see Figure 2a). Further showing that it is a problem of feature distribution not feature quality.

Lastly, we would like to emphasize that while having a dense ID representation can be important for OOD detection with clean ID data, it is much more important in the presence of pollution in the ID data. In this polluted setup, some OOD data are mixed in during training and considered ID by the loss. In this case, a compact ID data distribution decreases chance of other OOD data to be considered as ID as much as possible. This is empirically verified in the experimental section.

2.4 SIMSIAM AND BYOL GRADIENT FLOW PROBLEM

To avoid the degenerate solution of a collapsed representation, the authors of SimSiam (Chen & He, 2020) found it crucial to have a gradient blocking operation (`stop-grad`) that blocks gradients starting from \hat{z}_i from flowing back to other parts of the network. This lack of gradients acts as a regularizer and makes it hard for the optimizer to reach the trivial solution of a collapsed representation. Note that the same analysis presented here equally applies to BYOL (Grill et al., 2020b): the existence of the momentum encoder enforces an implicit `stop-grad`.

However both (Chen & He, 2020; Grill et al., 2020b) do not study the effect `stop-grad` may have on proper gradient flow in the network. Studying Figure 1, we can see that the l_2 -norm of the output of the prediction network $\hat{p}_i = p_i / \|p_i\|_2$ gives proper gradients that flows back to other parts of the network. The exact opposite happens for the l_2 -norm of the encoder network’s output: all gradients of that operation gets blocked by the `stop-grad`, though it is an integral part of the loss function.

Proposed solution Simply removing the `stop-grad` operation converges quickly to a collapsed representation (Chen & He, 2020). Another apparent straightforward solution is to minimize the norm of the output representation of the encoder f , but this limits the representation ability of the encoder and also rapidly collapses. One last trial would be removing normalization altogether in \mathcal{D} , however this converges to a sub-optimal representation with an unbounded norm (Grill et al., 2020b).

Our proposed solution is instead based on a simple observation. The missing gradient from \hat{z}_i carries two pieces of information: (a) moving the output of the encoder z_i to be closer to the output of the predictor p_i (which is the information we want to hide from the optimizer). (b) encouraging the projector g to learn a l_2 -norm invariant representation; this facilitates training the predictor network and thus also the encoder, and is what we want to maintain.

In order to maintain (b) while discarding (a), we propose a small modification (see Figure 1): we apply a differentiable l_2 -normalization to the projection z_i , such that the new projection is $\hat{z}_i = z_i / \|z_i\|_2$. This gives the network proper gradients for learning an l_2 -normalized representation satisfying the loss function \mathcal{D} while still having the `stop-grad` operation and avoiding related collapse.

2.5 FEATURE EVALUATION FOR OUT-OF-DISTRIBUTION DETECTION

Many recent works on OOD detection are based on scoring a given test sample using its distance to the nearest training sample (Tack et al., 2020; Schwag et al., 2021; Lee et al., 2018b). This provides a simple evaluation baseline with strong results. Many metrics have been used for this, the most commonly used are the Mahalanobis distance (Lee et al., 2018b; Schwag et al., 2021) and the Cosine distance (Tack et al., 2020) evaluated at the output of the network after the last convolutional block.

To take the advantages of both of these distances, we go a step further and score features with the arccosine of the Mahalanobis Cosine similarity (i.e. angular Mahalanobis distance) (Beveridge et al., 2005), which have been proposed and studied well previously in the field of face recognition (Beveridge et al., 2005; Vinay et al., 2015). Mahalanobis Cosine is the Cosine similarity between vectors after projection into the Mahalanobis space, where the famous Mahalanobis distance is the Euclidean distance computed between vectors after also projection into the Mahalanobis space.

If x_m, y are a training and test sample respectively, and the projection of their features $f(x_m), f(y)$ into the Mahalanobis space is u, v using the sample covariance matrix Σ_m and mean μ_m of the training data $\{x_m\}_{m=1}^M$, then the Mahalanobis Cosine distance \mathcal{D}_{MC} and our scoring \mathcal{S}_{k-Cos} are

$$u = \Sigma_m^{-1/2}(x_m - \mu_m), \quad \mathcal{D}_{MC}(x_m, y) = \frac{u \cdot v}{\|u\|_2 \cdot \|v\|_2}, \quad \mathcal{S}_{k-Cos}(y) = \arccos(\max_m \mathcal{D}_{MC}(x_m, y)) \quad (2)$$

\mathcal{S}_{k-Cos} considers only the distance to the nearest training sample and is used for most of our experiments. In Appendices C and G we study a variant \mathcal{S}_{c-Cos} , that is especially robust to pollution; it computes distance to μ_m , the mean vector of the training data $\{x_m\}$. $\mathcal{S}_{c-Cos}(y) = \arccos(\mathcal{D}_{MC}(\mu_m, y))$.

Feature ensembling We also propose another evaluation scheme where all the intermediate feature maps of the network are scored independently, then their scores are all summed together. The idea is to get both high level (from final layers) and low level (from initial layers) OOD scores using

different feature maps. Note that this is different from (Lee et al., 2018b) that learn a weighted sum of all the feature scores, where the weights are learned on a validation set; our proposed method is a simple sum and doesn’t need a validation set. It also attains a huge runtime saving when compared to test-time augmentation (TTA) used in (Tack et al., 2020) or model ensembling used in (Sohn et al., 2020), as it requires a single model forward pass on a single instance. It consists of three steps:

1. Computing a score for each feature map, using either \mathcal{S}_{k-Cos} or \mathcal{S}_{c-Cos} or both.
2. Normalizing the range of the scores to be between 0 and 1, using the range of training data scores.
3. Summing the normalized scores.

Due to space limitations we show detailed feature evaluation results in Appendix C, along with comparing different evaluation metrics. We then show extensive ablations in Appendix G. In Section 3.2, we firstly consider experimental results without ensembling, before comparing to methods that use ensembling in Section 3.2.4. Any result that includes ensembling strictly has the E suffix, which indicates using the *Ens.* combination whose components are precisely described in Appendix C.

3 EMPIRICAL EVALUATION

3.1 EXPERIMENTAL SETUP

We perform a thorough evaluation of our proposed normalization modifications on SimSiam, BYOL, and SimCLR (with and without negative / shifted augmentations). The problem discussed in Section 2.4 doesn’t apply to SimCLR (there is no stop-grad), so while both modifications are applied to SimSiam, our normalized variant of SimCLR only includes the change proposed in Section 2.3 for \hat{y} .

We evaluate in the one-vs-all OOD detection setting for CIFAR-10, CIFAR-100 super-classes (Krizhevsky et al., 2009), Fashion-MNIST (Xiao et al., 2017), and SVHN (Netzer et al., 2011). In this setting one class is treated as the normal class and the rest are treated as outliers.

For all results presented we use a ResNet-18, trained with Adam (Kingma & Ba, 2014) with a learning rate of 0.0001 and a cosine learning rate decay (Loshchilov & Hutter, 2016). For SimCLR we used 2-layer MLP as a projection head with an architecture similar to (Sohn et al., 2020). For SimSiam we used a 3-layer MLP for both the projector and the predictor. SimCLR is trained for 500 epochs, and SimSiam and BYOL for 4000 epochs. All models are trained on Nvidia V100 16GB GPUs and written in Pytorch (Paszke et al., 2019). All our reported results are without test-time augmentation.

For brevity, we often refer to SimSiam as **SS** and SimCLR as **SC**. Also **SS(n)**, **SC(n)** and **BYOL(n)** indicate inclusion of the proposed normalization, and **SC(-)** is with negative augmentations. Unless otherwise stated, our ensemble-free results use k-Cos Scoring. More details of the datasets, and additional comparisons/descriptions of competing methods can be found in Appendices B and F. An extensive ablation study including training 640 different models is provided in Appendix G.

3.2 RESULTS

3.2.1 ONE-CLASS CLASSIFICATION

Table 1 compares ensemble-free versions of our baselines BYOL, SimSiam, and SimCLR with and without normalization against current state of the art (without ensembling) DROC (Sohn et al., 2020), RotNet (Golan & El-Yaniv, 2018), and GOAD (Bergman & Hoshen, 2020). Extended comparison of our results (without ensembling) with many other published methods can be found in Appendix F.

We see that adding normalization is consistently effective across BYOL, SS, and SC in all scenarios. Also, SS(n) and BYOL(n) always achieve very competitive results compared to methods that use negative augmentations (SC(-) and DROC) while making much less assumptions about the underlying training data.

Data	p	BYOL	BYOL(n)	SS	SS(n)	SC	SC(n)	SC(-)	SC(n-)	RotNet	DROC	GOAD
C10	0	88.5	90.5	89.5	91.7	86.3	88.9	90.7	92.9	89.3	92.5	88.2
	0.1	82.9	85.3	83.2	86.3	65.6	79.8	79.6	83.9	78.5	80.5	83.0
C100	0	79.6	80.2	81.4	84.3	80.5	84.0	84.7	87.0	81.9	86.5	74.5
	0.1	76.2	77.8	78.9	80.3	75.9	80.0	80.5	82.8	-	-	-
fMNIST	0	95.3	95.1	95.9	95.0	94.6	94.9	94.7	95.7	94.6	94.5	94.1
	0.1	61.3	73.2	63.0	75.3	46.5	53.1	78.7	80.9	-	76.6	-

Table 1: Results of baselines and proposed variants compared to state of the art, without ensembling. p is the ratio of outlier pollution data inside the training set. **SS** is SimSiam, **SC** is SimCLR.

	BYOL(n) _E	SS(n) _E	SC(n) _E	SC(n-) _E	CSI	STOC
# Inference steps / example	1	1	1	1	160	1
# Trained models / class	1	1	1	1	1	60
Requires a good approximation of p	X	X	X	X	X	✓
Assumes rotation-variant data	X	X	X	✓	✓	✓

Data	p					
CIFAR10	0.0	91.9	92.5	90.3	93.0	94.3 92.1
	0.1	88.3	88.5	86.7	87.8	84.5 89.9
fMNIST	0.0	96.2	96.1	96.3	95.9	- 95.5
	0.1	87.9	87.8	87.5	90.9	- 85.7
CIFAR100	0.0	83.4	86.6		89.4	89.6 -
	0.1	80.7	82.5	83.0	85.7	- -

Table 2: Performance compared to state of the art under different ensembling setups. p is the ratio of outliers inside the training data.

3.2.2 PERFORMANCE UNDER POLLUTION

Table 1 also shows a comparison of the performance under the very realistic scenario that some $p\%$ of the training data are polluted with OOD data. It can be seen that adding the proposed normalization drastically reduces the effect of polluted data, and achieves state-of-the-art results (without ensembling).

One important take-away from the table is that, as predicted by our analysis in Section 2.3, positive only SSL (e.g. SS or BYOL) is much more suited to real world OOD detection which can possibly contain a small subset of polluted data compared to contrastive SSL (without negative augmentations) which suffers big performance drops in this scenario. In the case where negative augmentations are a suitable assumption, proposed SC(n-) gets even better results.

batch size	CIFAR10		CIFAR100	
	32	512	32	512
without norm	77.97	89.56	74.46	81.38
only normalize f	85.76	91.63	78.7	82.27
only normalize g	81.73	89.22	73.1	81.15
normalzie both	92.9	91.7	81.73	84.31

Table 3: An ablation of SimSiam showing the importance of both the normalization schemes proposed in Section 2.3 and 2.4, especially for in low batch-size training.

Trained from scratch		Pre-trained (1M images)				Pre-trained (1B images)	Pre-trained and adapted
		Supervised		Self-supervised			
SS(n)	SC(n)	PT R18	PT R50	PT R152	PT R50 (SC)	PT R50	PT R50
94.9	93.8	61	66	64	65	70	68

Table 4: OOD detection performance of various pre-trained backbones on SVHN

3.2.3 EFFECT OF NORMALIZATION

Table 3 examines the effect of the two proposed normalizations on SS on different batch size to assess the stability of training. As we can see for both batch-sizes both proposed normalizations do help the performance, and their combinations (proposed) is the best. We can also see for low batch sizes SS without norm suffers a big performance loss, which the proposed normalization fixes; this is a very important property as large batch training is not always an option.

3.2.4 EFFECT OF FEATURE ENSEMBLING

Table 2 shows results of the feature ensembling proposed in Section 2.5, compared to state-of-the-art techniques that also utilize ensembling: CSI (Tack et al., 2020) and STOC (Yoon et al., 2021). For fair comparison, we also state the relative computational budget (training or inference) for each. The proposed feature ensembles offer big computational savings compared to CSI and STOC at roughly the same scores. Lastly, improvements by ensembling are more significant when there are outliers in the training data.

3.2.5 PRETRAINED BACKBONES ON SVHN

Some concurrent works (Reiss & Hoshen, 2021; Fort et al., 2021) claim that ImageNet pre-trained models can act as a universal OOD detector and can work well on nearly any in-domain distribution. (Anonymous, 2022) showed that for classes not present in the pre-training data, pre-trained models perform poorly at OOD detection.

We confirm this here, and show that even for very simple datasets (e.g. SVHN) that require different kinds of discriminative features than those required for natural images, pre-trained models perform very poorly. Table 4 shows that regardless of the model size (ResNet 18 to 152) or size of pre-training dataset (from 1M images to 1B images (Yalniz et al., 2019)), or using fully-supervised or SSL pre-training, or even with state-of-the-art feature adaptation after pre-training (Reiss & Hoshen, 2021), all catastrophically fail at SVHN compared to training from scratch, which can get a nearly perfect score (we report other related pre-training results from our implementation in Appendix F, where as expected performance is good in situations the OOD task is similar enough to the pretraining dataset; we see this as not a truly practical OOD detection benchmark however).

4 CONCLUSION

We have considered a general framework to detection of Anomalies in images: using various SSL methods as deep feature extractors; followed by metric learning for outlier scoring. For each stage we have studied what does and doesn't work in a variety of scenarios, and proposed remedies and improvements that are also robust in the case of polluted training data and small batch sizes.

We have investigated and studied compactness of ID representation distributions as an important and very sensitive factor to the final OOD detection performance. Our experiments demonstrated that regardless of the quality of learned features, the ID representation compactness is critical. As its distribution gets closer to uniform, the OOD detection performance deteriorates significantly.

We have motivated, proposed, and studied an assumption-free, novel architectural modification for inducing this non-uniformity, and use it to solidly improve performance across contrastive and non-contrastive SSL-based OOD detection. We also studied several variants of feature scoring that work well across these different methods. More importantly, under the real world setting of totally unsupervised AD, where the ID training data can be polluted by some OOD outliers, our proposed modifications provide state-of-the-art performance among all competing methods.

Previous state-of-the-art literature for OOD detection was based on contrastive-based SSL with negative “distributionally-shifted” augmentations (e.g. 90 degree rotations). A big hurdle with the applicability of these methods is that the assumptions they make about the training data can be partially or fully invalid in real-world scenarios. Using our proposed “No Shifted Augmentations” (NSA) modifications, both contrastive and non-contrastive methods get a boost in their baseline performance, making them comparable to negative augmentation based techniques, but much more applicable to open world scenarios where little is controlled about ID data.

While model ensembling or Test-Time Augmentation is known in literature to be very effective for OOD, increased training/inference computational requirements can be often prohibitive. We went further and studied using light-weight multi-level feature ensembling for OOD. This enabled us to show state-of-the-art performance in terms of AUCROC, with huge savings in computational budget.

REFERENCES

- Anonymous. Improving and assessing anomaly detectors for large-scale settings. In *Submitted to The Tenth International Conference on Learning Representations*, 2022. URL <https://openreview.net/forum?id=vruwpl1pWnO>. under review.
- Arindam Banerjee, Inderjit S Dhillon, Joydeep Ghosh, Suvrit Sra, and Greg Ridgeway. Clustering on the unit hypersphere using von mises-fisher distributions. *Journal of Machine Learning Research*, 6(9), 2005.
- Liron Bergman and Yedid Hoshen. Classification-based anomaly detection for general data. In *International Conference on Learning Representations*, 2020.
- J Ross Beveridge, David Bolme, Bruce A Draper, and Marcio Teixeira. The csu face identification evaluation system. *Machine vision and applications*, 16(2):128–138, 2005.
- Ting Chen, Simon Kornblith, Mohammad Norouzi, and Geoffrey Hinton. A simple framework for contrastive learning of visual representations. In *International Conference on Machine Learning*, 2020a.
- Ting Chen, Simon Kornblith, Kevin Swersky, Mohammad Norouzi, and Geoffrey Hinton. Big self-supervised models are strong semi-supervised learners. *arXiv preprint arXiv:2006.10029*, 2020b.
- Xinlei Chen and Kaiming He. Exploring simple siamese representation learning. *arXiv preprint arXiv:2011.10566*, 2020.
- Hyunsun Choi, Eric Jang, and Alexander A Alemi. WAIC, but Why? Generative Ensembles for Robust Anomaly Detection. October 2018.
- Tim R Davidson, Luca Falorsi, Nicola De Cao, Thomas Kipf, and Jakub M Tomczak. Hyperspherical variational auto-encoders. *arXiv preprint arXiv:1804.00891*, 2018.
- Lucas Deecke, Robert A Vandermeulen, Lukas Ruff, Stephan Mandt, and Marius Kloft. Image Anomaly Detection with Generative Adversarial Networks. *ECML/PKDD*, 11051(3):3–17, 2018.
- Yilun Du and Igor Mordatch. Implicit generation and generalization in energy-based models. *CoRR*, 2019. URL <http://arxiv.org/abs/1903.08689v6>.
- Stanislav Fort, Jie Ren, and Balaji Lakshminarayanan. Exploring the limits of out-of-distribution detection. *arXiv preprint arXiv:2106.03004*, 2021.
- Izhak Golan and Ran El-Yaniv. Deep anomaly detection using geometric transformations. In *Advances in Neural Information Processing Systems*, 2018.
- Sachin Goyal, Aditi Raghunathan, Moksh Jain, Harsha Vardhan Simhadri, and Prateek Jain. Droc: Deep robust one-class classification. In *International Conference on Machine Learning*, pp. 3711–3721. PMLR, 2020.

-
- Will Grathwohl, Kuan-Chieh Wang, Jörn-Henrik Jacobsen, David Duvenaud, Mohammad Norouzi, and Kevin Swersky. Your classifier is secretly an energy based model and you should treat it like one. *CoRR*, 2019. URL <http://arxiv.org/abs/1912.03263v2>.
- Arthur Gretton, Karsten M Borgwardt, Malte J Rasch, Bernhard Schölkopf, and Alexander Smola. A kernel two-sample test. *The Journal of Machine Learning Research*, 13(1):723–773, 2012.
- Jean-Bastien Grill, Florian Strub, Florent Alché, Corentin Tallec, Pierre H Richemond, Elena Buchatskaya, Carl Doersch, Bernardo Avila Pires, Zhaohan Daniel Guo, Mohammad Gheshlaghi Azar, Bilal Piot, Koray Kavukcuoglu, Remi Munos, and Michal Valko. Bootstrap Your Own Latent: A New Approach to Self-Supervised Learning. June 2020a.
- Jean-Bastien Grill, Florian Strub, Florent Alché, Corentin Tallec, Pierre H Richemond, Elena Buchatskaya, Carl Doersch, Bernardo Avila Pires, Zhaohan Daniel Guo, Mohammad Gheshlaghi Azar, et al. Bootstrap your own latent: A new approach to self-supervised learning. *arXiv preprint arXiv:2006.07733*, 2020b.
- Sungwon Han, Hyeonho Song, Seungeon Lee, Sungwon Park, and Meeyoung Cha. Elsa: Energy-based learning for semi-supervised anomaly detection. *arXiv preprint arXiv:2103.15296*, 2021.
- Md Hasnat, Julien Bohné, Jonathan Milgram, Stéphane Gentric, Liming Chen, et al. von mises-fisher mixture model-based deep learning: Application to face verification. *arXiv preprint arXiv:1706.04264*, 2017.
- K He, Kaiming He, Haoqi Fan, H Fan, Yuxin Wu, Y Wu, S Xie, Saining Xie, R Girshick arXiv preprint arXiv 1911.05722, Ross Girshick, and 2019. Momentum Contrast for Unsupervised Visual Representation Learning. *arXiv.org*, November 2019.
- Dan Hendrycks, Mantas Mazeika, Saurav Kadavath, and Dawn Song. Using self-supervised learning can improve model robustness and uncertainty. In *Advances in Neural Information Processing Systems*, pp. 15663–15674, 2019.
- Chaoqin Huang, Fei Ye, Jinkun Cao, Maosen Li, Ya Zhang, and Cewu Lu. Attribute Restoration Framework for Anomaly Detection. November 2019.
- Diederik P Kingma and Jimmy Ba. Adam: A method for stochastic optimization. *arXiv preprint arXiv:1412.6980*, 2014.
- Durk P Kingma and Prafulla Dhariwal. Glow: Generative flow with invertible 1x1 convolutions. In *Advances in Neural Information Processing Systems*, 2018.
- Alex Krizhevsky et al. Learning multiple layers of features from tiny images, 2009.
- Sachin Kumar and Yulia Tsvetkov. Von mises-fisher loss for training sequence to sequence models with continuous outputs. *arXiv preprint arXiv:1812.04616*, 2018.
- Cheolhyoung Lee, Kyunghyun Cho, and Wanmo Kang. Directional analysis of stochastic gradient descent via von mises-fisher distributions in deep learning. *arXiv preprint arXiv:1810.00150*, 2018a.
- Kimin Lee, Kibok Lee, Honglak Lee, and Jinwoo Shin. A simple unified framework for detecting out-of-distribution samples and adversarial attacks. In *Advances in Neural Information Processing Systems*, 2018b.
- Kuang-Huei Lee, Anurag Arnab, Sergio Guadarrama, John Canny, and Ian Fischer. Compressive visual representations. *arXiv preprint arXiv:2109.12909*, 2021.
- Chun-Liang Li, Kihyuk Sohn, Jinsung Yoon, and Tomas Pfister. Cutpaste: Self-supervised learning for anomaly detection and localization. *arXiv preprint arXiv:2104.04015*, 2021.
- Ilya Loshchilov and Frank Hutter. Sgdr: Stochastic gradient descent with warm restarts. *arXiv preprint arXiv:1608.03983*, 2016.
- Ishan Misra and Laurens van der Maaten. Self-Supervised Learning of Pretext-Invariant Representations. December 2019.

-
- Eric Nalisnick, Akihiro Matsukawa, Yee Whye Teh, Dilan Gorur, and Balaji Lakshminarayanan. Do Deep Generative Models Know What They Don't Know? October 2018.
- Yuval Netzer, Tao Wang, Adam Coates, Alessandro Bissacco, Bo Wu, and Andrew Y. Ng. Reading digits in natural images with unsupervised feature learning. In *Advances in Neural Information Processing Systems Workshop on Deep Learning and Unsupervised Feature Learning*, 2011.
- Mehdi Noroozi and Paolo Favaro. Unsupervised Learning of Visual Representations by Solving Jigsaw Puzzles. March 2016.
- Aaron van den Oord, Yazhe Li, and Oriol Vinyals. Representation learning with contrastive predictive coding. *CoRR*, 2018. URL <http://arxiv.org/abs/1807.03748v2>.
- Tianyu Pang, Kun Xu, Yinpeng Dong, Chao Du, Ning Chen, and Jun Zhu. Rethinking softmax cross-entropy loss for adversarial robustness. *arXiv preprint arXiv:1905.10626*, 2019.
- Adam Paszke, Sam Gross, Francisco Massa, Adam Lerer, James Bradbury, Gregory Chanan, Trevor Killeen, Zeming Lin, Natalia Gimelshein, Luca Antiga, et al. Pytorch: An imperative style, high-performance deep learning library. *arXiv preprint arXiv:1912.01703*, 2019.
- Pramuditha Perera, Ramesh Nallapati, and Bing Xiang. OCGAN: One-class Novelty Detection Using GANs with Constrained Latent Representations. March 2019.
- Stanislav Pidhorskyi, Ranya Almohsen, Donald A Adjeroh, and Gianfranco Doretto. Generative Probabilistic Novelty Detection with Adversarial Autoencoders. July 2018.
- Tal Reiss and Yedid Hoshen. Mean-shifted contrastive loss for anomaly detection. *arXiv preprint arXiv:2106.03844*, 2021.
- Tal Reiss, Niv Cohen, Liron Bergman, and Yedid Hoshen. PANDA: Adapting Pretrained Features for Anomaly Detection and Segmentation. October 2020.
- Douglas A Reynolds. Gaussian mixture models. *Encyclopedia of biometrics*, 741:659–663, 2009.
- Oliver Rippel, Patrick Mertens, and Dorit Merhof. Modeling the Distribution of Normal Data in Pre-Trained Deep Features for Anomaly Detection. May 2020.
- Lukas Ruff, Robert Vandermeulen, Nico Goernitz, Lucas Deecke, Shoaib Ahmed Siddiqui, Alexander Binder, Emmanuel Müller, and Marius Kloft. Deep one-class classification. In *International conference on machine learning*, pp. 4393–4402. PMLR, 2018.
- Lukas Ruff, Robert A Vandermeulen, Billy Joe Franks, Klaus-Robert Müller, and Marius Kloft. Rethinking assumptions in deep anomaly detection. In *ICML 2021 Workshop on Uncertainty & Robustness in Deep Learning*, 2021.
- Thomas Schlegl, Philipp Seeböck, Sebastian M Waldstein, Ursula Schmidt-Erfurth, and Georg Langs. Unsupervised Anomaly Detection with Generative Adversarial Networks to Guide Marker Discovery. March 2017.
- Ludwig Schmidt, Shibani Santurkar, Dimitris Tsipras, Kunal Talwar, and Aleksander Madry. Adversarially robust generalization requires more data. *arXiv preprint arXiv:1804.11285*, 2018.
- Bernhard Schölkopf, Robert C Williamson, Alex J Smola, John Shawe-Taylor, and John C Platt. Support vector method for novelty detection. In *Advances in Neural Information Processing Systems*, 2000.
- Vikash Sehwal, Mung Chiang, and Prateek Mittal. {SSD}: A unified framework for self-supervised outlier detection. In *International Conference on Learning Representations*, 2021. URL <https://openreview.net/forum?id=v5gjXpmR8J>.
- Kihyuk Sohn, Chun-Liang Li, Jinsung Yoon, Minho Jin, and Tomas Pfister. Learning and evaluating representations for deep one-class classification. *arXiv preprint arXiv:2011.02578*, 2020.
- Suvrit Sra. A short note on parameter approximation for von mises-fisher distributions: and a fast implementation of $i s(x)$. *Computational Statistics*, 27(1):177–190, 2012.

-
- Jihoon Tack, Sangwoo Mo, Jongheon Jeong, and Jinwoo Shin. CSI: Novelty detection via contrastive learning on distributionally shifted instances. *Advances in Neural Information Processing Systems*, 33:11839–11852, 2020.
- Yu Tian, Guansong Pang, Fengbei Liu, Seon Ho Shin, Johan W Verjans, Rajvinder Singh, Gustavo Carneiro, et al. Constrained contrastive distribution learning for unsupervised anomaly detection and localisation in medical images. *arXiv preprint arXiv:2103.03423*, 2021.
- A Vinay, Vinay S Shekhar, KN Balasubramanya Murthy, and S Natarajan. Performance study of lda and kfa for gabor based face recognition system. *Procedia Computer Science*, 57:960–969, 2015.
- Tongzhou Wang and Phillip Isola. Understanding contrastive representation learning through alignment and uniformity on the hypersphere. In *International Conference on Machine Learning*, pp. 9929–9939. PMLR, 2020.
- Jim Winkens, Rudy Bunel, Abhijit Guha Roy, Robert Stanforth, Vivek Natarajan, Joseph R Ledsam, Patricia MacWilliams, Pushmeet Kohli, Alan Karthikesalingam, and Simon Kohl. Contrastive training for improved out-of-distribution detection. *arXiv preprint arXiv:2007.05566*, 2020.
- Zhirong Wu, Yuanjun Xiong, Stella X Yu, and Dahua Lin. Unsupervised feature learning via non-parametric instance discrimination. In *IEEE Conference on Computer Vision and Pattern Recognition*, 2018.
- Han Xiao, Kashif Rasul, and Roland Vollgraf. Fashion-mnist: a novel image dataset for benchmarking machine learning algorithms. *arXiv preprint arXiv:1708.07747*, 2017.
- Zhisheng Xiao, Qing Yan, and Yali Amit. Do We Really Need to Learn Representations from In-domain Data for Outlier Detection? May 2021.
- I Zeki Yalniz, Hervé Jégou, Kan Chen, Manohar Paluri, and Dhruv Mahajan. Billion-scale semi-supervised learning for image classification. *arXiv preprint arXiv:1905.00546*, 2019.
- Jinsung Yoon, Kihyuk Sohn, Chun-Liang Li, Serkan O Arik, Chen-Yu Lee, and Tomas Pfister. Self-trained one-class classification for unsupervised anomaly detection. *arXiv preprint arXiv:2106.06115*, 2021.
- Shuangfei Zhai, Yu Cheng, Weining Lu, and Zhongfei Zhang. Deep structured energy based models for anomaly detection. In *International Conference on Machine Learning*, 2016.
- Richard Zhang, Phillip Isola, and Alexei A Efros. Colorful image colorization. In *European Conference on Computer Vision*, 2016.
- Bo Zong, Qi Song, Martin Renqiang Min, Wei Cheng, Cristian Lumezanu, Daeki Cho, and Haifeng Chen. Deep Autoencoding Gaussian Mixture Model for Unsupervised Anomaly Detection. February 2018.

A PLOTS FOR EVALUATIONS DURING TRAINING

Here we show the detailed version of the summary (mean) plots presented in Figure 2 in the main text. They show the same curves for 4 distinct classes of CIFAR10, and also under 3 different metrics. They appear in Figure 3 (SimCLR AUC and Linear probes during training), Figure 4 (SimCLR Kappa and MMD during training), Figure 5 (SimSiam AUC during training), Figure 6 (SimSiam Kappa and MMD during training), and Figure 7 (SimCLR with norm AUC). The same findings as in the main text are seen to hold across these detailed variants.

B DATASET DETAILS

The main datasets we test on are: CIFAR 10, CIFAR 100 and ImageNet30, fashion-MNIST following the splits and protocols specified in (Tack et al., 2020) and (Sohn et al., 2020); we add SVHN using the same basic protocol of one class as inlier v.s. the remaining as outliers. We resized images to 32 x 32 for all datasets apart from ImageNet30 which uses the standard ImageNet ResNet-18 architecture’s transformation of a 224-pixel center-cropped region from the 256 x 256 input image.

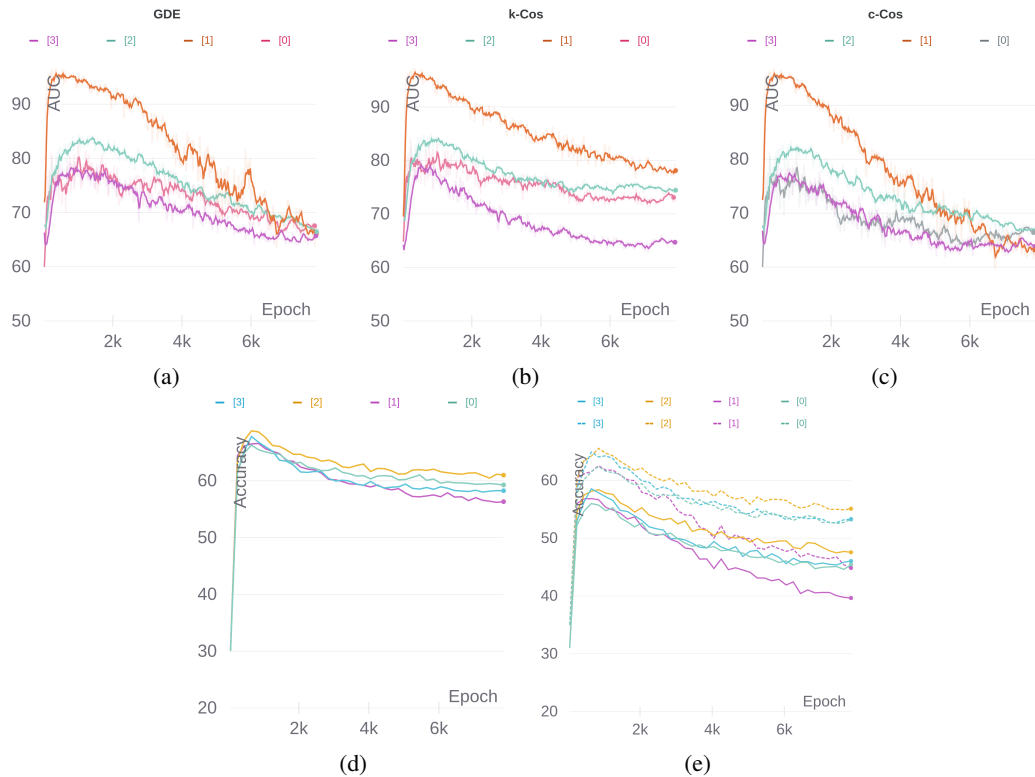


Figure 3: Training SimCLR on classes 0,1,2,3 from CIFAR10 and evaluating the representation during training. (a) Using Gaussian density estimation (GDE) (Reynolds, 2009). (b) k -Cos cosine distance to the closest ($k=1$) point in ID data. (c) c -Cos cosine distance to the mean direction in ID data. Both these are defined in more detail in section 2.5. (d) Linear evaluation (Zhang et al., 2016) of learned embedding. (e) Weighted nearest neighbor classifier (k-NN) (Wu et al., 2018). Solid lines represent $k = 1$ and dashed lines represent $k = 20$

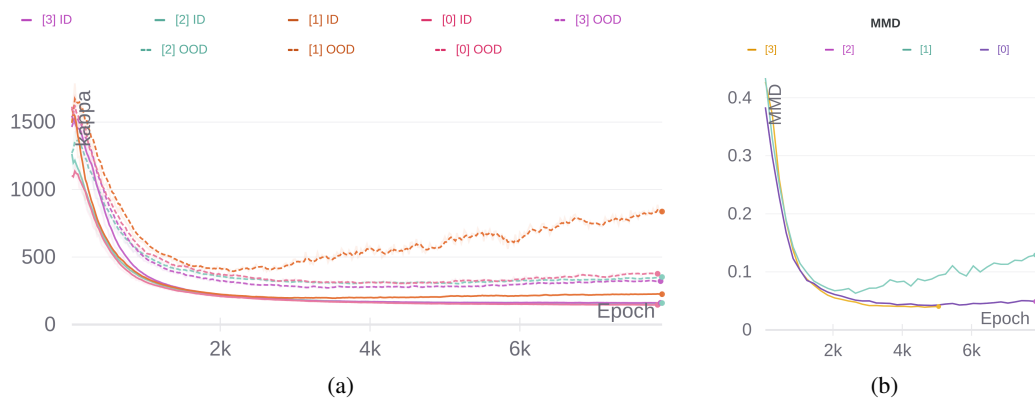


Figure 4: Training SimCLR on classes 0,1,2,3 from CIFAR10 and monitoring the learned vMF ID and OOD representations during training. (a) κ progress during training; solid lines are ID data and dashed are OOD data. (b) The MMD (Gretton et al., 2012) between the learned representation and samples from uniform distribution on a unit hypersphere (lower is more uniform).

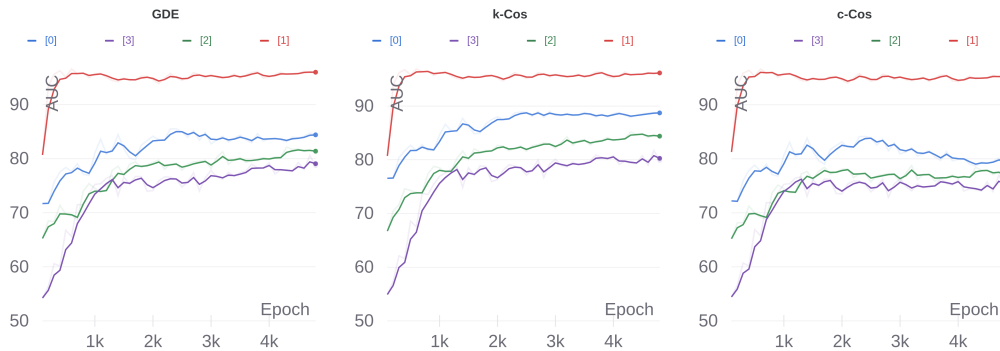


Figure 5: Same experiment as Figure 3 but with SimSiam.

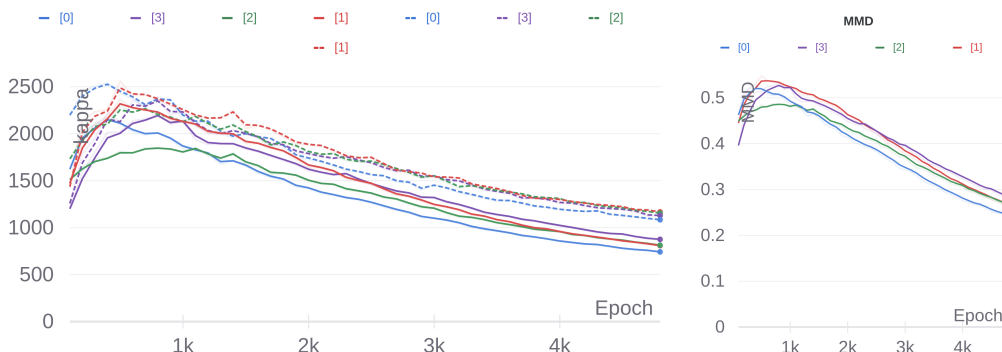


Figure 6: Same experiment as Figure 4 but with SimSiam.

C COMPARISON OF SCORING WITH DIFFERENT FEATURE EVALUATIONS, METRICS & ENSEMBLING

As discussed in Section 2.5, we compare the default scoring used in our main experiments (the encoder’s last layer features using \mathcal{S}_{k-Cos}) with a feature ensembling evaluation scheme consisting of these scores summed across feature maps from the encoder backbone network, and projection heads from either SimSiam or SimCLR. In the following tables we use following feature maps:

- `conv_block_n`: The output feature map from block n of the convolutional backbone. Which is first directly flattened from 2D to 1D before evaluation.
- `conv_block_n (1x1)`: Same as `conv_block_n` but after pooling to a size of 1x1.
- `head_layer_n`: The output feature map from layer n of the projection head.
- `All Conv blocks`: The sum of the scores of all convolutional blocks, using the distance specified in column, then summed across table columns merged in table.
- `All blocks`: The sum of the scores of all network internal feature maps, using the distance specified in column, then summed across table columns merged in table.
- `Ens.:` The sum of $k-Cos$ and $k-Cos (Mah)$ for 2D feature maps (e.g. convolutional feature maps) and $c-Cos$ and $c-Cos (Mah)$ for 1D feature maps (e.g. projection heads).

We also investigate 5 different metric functions for computing the OOD score, namely:

- $k-Cos$: Cosine distance to closest ($k=1$) training vector, introduced in Section 2.5
- $k-Cos (Mah)$: Same but evaluated in Mahalanobis space.
- $c-Cos$: Cosine distance to the mean of all the training set vectors, introduced in Section 2.5.
- $c-Cos (Mah)$: Same but evaluated in Mahalanobis space.

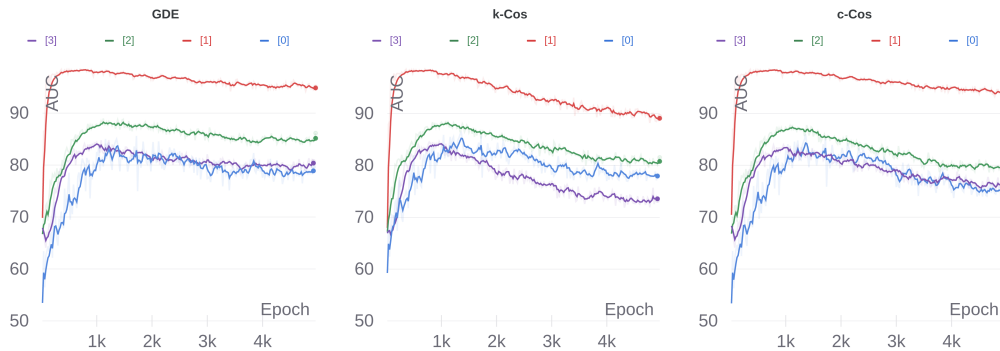


Figure 7: Same experiment as Figure 3 but after adding the normalization proposed in Section 2.3.

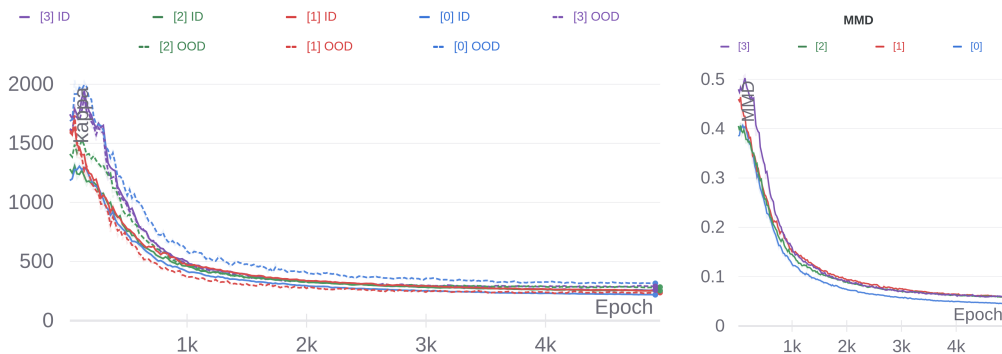


Figure 8: Same experiment as Figure 4 but after adding the normalization proposed in Section 2.3.

- *GDE*: A Gaussian Kernel density estimator, we use the same configuration as in Sohn et al. (2020).

Tables 6,7,8 show an extensive evaluation of presented models at most internal layers and a variety of scoring metrics. We should highlight the fact that each number presented in those tables is the average across all classes in the dataset, with one experiment per class i.e. 10 experiments for CIFAR10, and 20 experiments for CIFAR100. We can notice:

- The Cosine Mahalanobis distance mostly outperforms most other evaluation metrics, sometimes a by large gap.
- There is a consistent improvement associated with ensembling of feature scores. This is true across models and across datasets.
- We note this type of feature ensembling can be considered free, computation-wise, compared with the ensembling used in e.g. CSI, that slows down the method significantly at inference.

D CIFAR 10 PER-CLASS RESULTS

Here in Table 9 we show the per class results for each of the CIFAR 10 classes trained for one-class classification against the others, and compare our NSA method (SimSIAM with Norm, no ensembling augmentations), with (i) last layer features only and (ii) summing all features, with other recent works that also report these results.

E ADDITIONAL POLLUTION RESULTS

Table 10 shows additional CIFAR10 results in the presence of pollution, also more comparisons.

		CIFAR10	CIFAR100	IN30	fMNIST	SVHN
Ours	1. SS(n) = SimSiam with norm, aka “NSA”	91.54	84.09	80.88	95.15	94.91
	2. SC(n) = SimCLR(w norm, no neg aug)	89.27	83.95	75.17	94.61	93.84
	3. SC = SimCLR(w/o norm, no neg aug)	86.49	80.51	75.17	94.61	93.84
	4. SS(-) = SimCLR(w/o norm, neg aug)	91.12	86.68	76.97	95.47	92.17
Pretraining / FT	5. Pretrained ResNet18* [Ours]	93.63	92.64	99.78	94.35	61.06
	6. Pretrained ResNet50* [Ours]	94.45	94.68	99.91	95.16	66.28
	7. Pretrained ResNet152* [Ours]	95.82	95.21	99.96	94.99	63.41
	8. PT ResNet50 (DROC (Sohn et al., 2020))*	80.0	83.7	-	91.8	-
	10. ResNet152 (DN2 (Reiss et al., 2020))*	92.5	94.1	-	94.5	-
	11. ResNet152 (PANDA (Reiss et al., 2020))*	96.2	94.1	-	95.6	-
12. Self-Sup. PT R50. Xiao et al.(Xiao et al., 2021)*	93.8	92.6	-	94.4	-	
Dist. Shifting	13. CSI (SimCLR loss only)**	87.9	-	-	-	-
	13. CSI (SimCLR w neg aug only)**	90.1	86.5	83.1	-	-
	14. CSI (Full)**	94.3	89.6	91.6	-	-
	15. DROC, Contrastive	89.0	82.4	-	93.9	-
16. DROC, Contrastive DA	92.5	86.5	-	94.8	-	
Other Methods	19. DeepSVDD (Ruff et al., 2018)	64.8	67.0	-	84.8	-
	20. DROCC (Goyal et al., 2020)	74.2	-	-	-	-
	21. Geom (Golan et al.) (Golan & El-Yaniv, 2018)**	86.0	78.7	-	93.5	-
	22. GOAD (Bergman) (Bergman & Hoshen, 2020)**	88.2	74.5	-	94.1	-
	23. ARNet (Huang) (Huang et al., 2019)**	86.6	78.8	-	93.33	-
	24. Hendrycks et al. (Hendrycks et al., 2019)**	90.1	79.8	85.7	93.2	-
	25.SSD (Sehwag et al., 2021)	90.0	-	-	-	-

Table 5: One-Class Classification Summary results reported in the literature on various datasets, plus some of our results; all figures are AUC. * indicates methods trained on external additional data, which may overlap in scope with the “unseen” OOD data. ** indicates method using test-time data augmentation / ensembling during evaluation, which can involve drastically slower inference.

	k-Cos	k-Cos (Mah)	c-Cos	c-Cos (Mah)	GDE
conv_block_2	80.29	83.58	65.35	83.52	
conv_block_3	85.87	83.59	75.81	83.53	
conv_block_4	92.21	91.20	88.35	91.12	
conv_block_1 (1x1)	71.29	70.85	68.39	67.37	67.39
conv_block_2 (1x1)	73.19	71.93	70.94	69.66	69.39
conv_block_3 (1x1)	81.46	83.47	73.60	79.66	79.32
conv_block_4 (1x1)	91.85	91.54	84.88	90.52	91.04
head_layer_1	82.64	87.84	71.18	87.56	
head_layer_2	80.62	83.08	70.50	82.76	
head_layer_3	79.67	77.41	51.93	54.64	
All Conv blocks	92.37		90.79		
All Conv blocks	92.01				
All blocks	91.62	92.23	80.50	90.86	89.96
All blocks	92.86		88.74		
All blocks	92.86				
Ens.	92.5				

Table 6: Different feature ensembling methods: SimSiam w norm on Cifar10. Note that items spanning multiple columns imply summation of the corresponding features.

	k-Cos	k-Cos (Mah)	c-Cos	c-Cos (Mah)	GDE
conv_block_2	73.36	76.42	58.54	76.39	
conv_block_3	79.31	77.83	68.39	77.80	
conv_block_4	85.47	84.46	78.19	84.40	
conv_block_1 (1x1)	66.35	67.51	60.75	64.77	64.76
conv_block_2 (1x1)	68.05	67.99	61.93	65.46	65.37
conv_block_3 (1x1)	74.26	76.49	64.76	72.78	72.75
conv_block_4 (1x1)	84.76	84.09	72.08	82.74	83.15
head_layer_1	76.95	81.46	64.50	81.24	
head_layer_2	74.78	77.46	62.95	77.29	
head_layer_3	75.23	73.86	52.65	68.15	
All Conv blocks	86.45		84.75		
All Conv blocks	85.89				
All blocks	85.19	87.11	72.50	86.17	
All blocks	87.54		85.79		
All blocks	87.25				
Ens.	86.6				

Table 7: Different feature ensembling methods: SimSiam w norm on Cifar100

	k-Cos	k-Cos (Mah)	c-Cos	c-Cos (Mah)	GDE
conv_block_2	79.62	82.40	64.71	82.32	
conv_block_3	81.08	80.22	73.38	80.14	
conv_block_4	88.92	89.47	82.83	89.42	
conv_block_1 (1x1)	71.63	71.53	68.56	68.12	68.17
conv_block_2 (1x1)	73.85	72.67	70.60	70.12	69.79
conv_block_3 (1x1)	74.97	77.00	68.97	74.47	73.50
conv_block_4 (1x1)	86.68	89.27	75.68	88.43	88.39
head_layer_1	73.88	81.05	48.36	80.63	
head_layer_2	65.19	72.33	41.26	46.18	
All Conv blocks	90.65		89.61		
All Conv blocks	90.57				
All blocks	87.37	90.16	75.65	89.12	
All blocks	90.20		89.10		
All blocks	90.35				
Ens.	90.3				

Table 8: Different feature ensembling methods: SimCLR w norm on Cifar10

	Plane	Car	Bird	Cat	Deer	Dog	Frog	Horse	Ship	Truck	Mean
CSI (Tack et al., 2020), inc. ensembling augmentations	90.0	99.1	93.2	86.4	93.8	93.4	95.2	98.6	97.9	95.5	94.3
DROC, OC-SVM (Sohn et al., 2020)	88.8	97.5	87.7	82.0	82.4	89.2	89.7	95.6	86.0	90.6	89.0
DROC OC-SVM (DA) (Sohn et al., 2020)	91.0	98.9	88.0	83.2	89.4	90.0	93.5	98.1	96.5	95.1	92.5
DROC Gaussian KDE (DA) (Sohn et al., 2020)	91.0	98.9	88.0	83.2	89.4	90.2	93.5	98.1	96.5	95.1	92.4
Rot. Pred. OC-SVM, from (Sohn et al., 2020)	83.6	96.9	87.9	79.0	90.5	89.5	94.1	96.7	95.0	94.9	90.8
Denosing OC-SVM, from (Sohn et al., 2020)	81.6	92.4	75.9	72.3	82.3	83.1	86.7	91.2	78.0	91.0	83.4
RotNet Rot. Cls. (Golan & El-Yaniv, 2018)	80.3	91.2	85.3	78.1	85.9	86.7	89.6	93.3	91.8	86.0	86.8
NSA (SimSIAM w norm) [Ours]	90.4	98.6	85.2	85.7	84.1	92.9	92.9	94.5	96.3	90.99	91.52
NSA (SimSIAM w norm) All features [Ours]	93.07	98.44	87.16	83.81	90.34	91.79	96.79	96.16	94.80	96.29	92.86

Table 9: CIFAR10 Per class results

	p=0	p=0.05	p=0.10	Δ (p=0.1 - p=0)
SimSiam(w norm)	91.54	88.08	86.21	5.33
SimSiam(w/o norm)	89.56	85.21	81.79	7.77
SimCLR(no neg, w norm)	89.27	83.1	77.49	11.78
SimCLR(no neg, w/o norm)	86.49	71.1	63.5	25.99
SimCLR (neg aug, w norm)	92.91	86.1	83.38	9.53
SimCLR (neg aug, w/o norm)	91.12	81.5	77.94	13.18
Pretrained IN18	92.63	90.9	89.3	3.33
Pretrained IN50	94.45	92.18	89.49	4.96
Pretrained IN152	95.82	94.48	91.39	4.43
DROC (Sohn et al., 2020)	89	76.5	73.0	16.0
DROC (DA) (Sohn et al., 2020)	92.5	85.0	80.5	12.0
CSI (results from (Han et al., 2021))	94.3	88.2	84.5	9.8
Semi-Supervised (5% labeled) ELSA (Han et al.)	85.7	83.5	81.6	4.1
Semi-Supervised (5% labeled) ELSA+ (Han et al.)	95.2	93.0	91.1	4.1

Table 10: CIFAR10 pollution experiments. p is the ratio of outlier data inside the training set. the last column is the loss in performance between training with clean data and a 10% polluted data. Clearly, our proposed modifications reduces the drop in all cases. With SimSiam we beat standard ELSA which uses 5% labeled data to maintain robustness to pollution, and come close to ELSA+, which uses TTA and other tricks from CSI on top of the baseline SSL approach.

F ADDITIONAL COMPARISON WITH PREVIOUS RESULTS FROM LITERATURE

Table 5 gives a more detailed overview of related OOD / One Class Classification results from the literature, and comparison with variants of our baseline (ensemble free) variants of SimSiam, SimCLR, along with our implementation of pretrained ResNets (as an additional baseline for comparison to other pretrained methods).

The pretrained results also serve to indicate where these types of approaches can fall down, and the issues in a with fairly comparing these pretrained methods with from-scratch trained approaches in the Anomaly/OOD detection context (It is unsurprising that pretraining a representation on ImageNet does well at distinguishing “unseen” ImageNet30 classes in a One-Class classifier scenario, and similarly for e.g. CIFAR, where the same types of class are present; however SVHN is less similar and therefore the pretrained representation is less useful).

More details and notes on these competing methods follow. In particular, we clarify that “(n)” indicates a method using our proposed modifications, and “w/o norm” is the standard version of the architecture (SimCLR or SimSiam) without these modifications. “(-)” means including strong distributionally negative shifted augmentations, using randomly the four 0, 90, 180, and 270 degree rotations, following the approach of CSI (Tack et al., 2020).

We note in particular that CSI’s method combines many parts (contrastive+classification losses and scoring functions, plus ensembling) which each contribute something and add up to give good results. Our goal of instead showing baseline SimCLR results with / without the norm, and with/without shifted augmentations is to create a more straightforward baseline to compare with. We note improved results are possible with our method adding these additional features such as ensembling, but also at additional computational cost, as is the case with CSI.

On the other hand, our pretrained baselines obtain very good results equal or exceeding PANDA (Reiss et al., 2020)’s fine-tuned results on datasets that are similar in nature to ImageNet that they are pretrained on; this exemplifies the benefits of our chosen scoring metric $\mathcal{S}_{NSA} = \mathcal{S}_{k-Cos}$ on good representations in general. However we also show datasets where this approach falls down, compared with self-supervised methods.

For each of the methods, here is a more detailed description of the features, networks, scoring functions etc. used for comparison:

-
1. NSA [ours]; features = SimSiam (with norm), ResNet18; scoring = KNN + Mahalanobis Cosine, last layer features.
 2. features = SimCLR(w norm) + **NO** negative shifting augmentations, ResNet18 ; scoring = KNN + Mahalanobis Cosine, last layer features. [our baseline]
 3. features = SimCLR(w/o norm) + **NO** negative shifting augmentations, ResNet18 ; scoring = KNN + Mahalanobis Cosine, last layer features. [our baseline]
 4. features = SimCLR(w/o norm) + **With** strong rotation negative shifting augmentations, ResNet18; scoring = KNN + Mahalanobis Cosine, last layer features [our baseline, closest to CSI (**without ensembling**) / DROC+DA]
 5. Pretrained ResNet18 (on ImageNet), **no fine-tuning**; scoring = KNN + Mahalanobis Cosine, last layer features [our baseline]
 6. Pretrained ResNet50 (on ImageNet), **no fine-tuning**; scoring = KNN + Mahalanobis Cosine, last layer features [our baseline]
 7. Pretrained ResNet152 (on ImageNet), **no fine-tuning**; scoring = KNN + Mahalanobis Cosine, last layer features [our baseline]
 8. Pretrained ResNet-50 on ImageNet, results from DROC (Sohn et al., 2020)
 9. Rippel et al. (Rippel et al., 2020) - Pretrained EfficientNet-B4 on Imagenet + Mahalanobis (no results on our benchmark datasets).
 10. Reiss et al (Reiss et al., 2020) Simple baseline “DN2” - Pretrained ResNet-152 on ImageNet, **no fine-tuning** + kNN=2 scoring from last layer, presumably euclidean distance
 11. Reiss et al. (Reiss et al., 2020) PANDA-EWC - Pretrained ResNet-152 on ImageNet, **Fine-tuned** last 2 layers on each dataset, with compactness loss + kNN=2 scoring from last layer, presumably euclidean distance.
 12. Xiao et al.(Xiao et al., 2021) - Self-supervised Pretrained ResNet-50. SimCLRv2, Gaussian Mixture Model / Mahalanobis distance .
 13. (a) CSI, SimCLR loss only; features = SimCLR (w/o norm), ResNet18 ; scoring = Sim-only contrastive(cosine * norm). [their results Table 15]; (b) same but with full CSI loss, contrastive **With** strong rotation negative shifting augmentations; scoring = contrastive Sim-only (cosine).
 14. Full CSI; features = SimCLR(w/o norm) + **With** strong rotation negative shifting augmentations, ResNet18 ; scoring = contrastive(cosine * norm) + rotation prediction, on shifted transforms, **with ensembles**. [their main results, essentially combining many parts]
 15. DROC (Sohn et al., 2020) Contrastive (=Deep Representation One-class Classification); features = SimCLR(w/o norm) + **NO** negative shifting augmentations ; scoring = (OC-SVM). [their results]
 16. DROC (Sohn et al., 2020) Contrastive DA (=Deep Representation One-class Classification); features = SimCLR(w/o norm) + **With** strong rotation negative shifting augmentations ; scoring = (OC-SVM). [their results]
 17. ELSA (Han et al., 2021) - **NO** negative shifting augmentations - with 1% labeled outliers (Han et al., 2021)
 18. ELSA+ (Han et al., 2021) - **With** strong rotation negative shifting augmentations (like CSI), and **with ensembles** - also with 1% labeled outliers (Han et al., 2021)
 19. DeepSVDD, Ruff et al. (Ruff et al., 2018), with LeNet architecture Autoencoder + adapted features. [All results apart from CIFAR10 from Reiss(Reiss et al., 2020)]
 20. DROCC, Goyal et al. (Goyal et al., 2020) - LeNet architecture
 21. Geom - Golan et al. (Golan & El-Yaniv, 2018) - WRN-16-8 Arch.
 22. GOAD, Bergman et al. (Bergman & Hoshen, 2020) - WRN-16-4 architecture [CIFAR 100 results from CSI with ResNet18] (Bergman & Hoshen, 2020)
 23. ARNet (formerly called Inv. Trans AE) - Huang et al Huang et al. (2019)
 24. Rot + Trans, Hendrycks et al. (Hendrycks et al., 2019) - WRN-16-4 architecture (CIFAR 100 results from CSI with ResNet18; IN30 are ResNet18 Rot+Trans+Attn+Resize; fMNIST results from Reiss (Reiss et al., 2020))

-
25. SSD (Sehwag et al., 2021); features = SimCLR(w/o norm) + **NO** negative shifting augmentations ; scoring = Mahalanobis [their results]

G DETAILED ABLATION STUDY

In Table 11 we show an extensive ablation study demonstrating results on CIFAR10, CIFAR100 and fMNIST of each variant of the methods we study, with and without our normalization enhancements, for different pollution settings, and under 5 different feature evaluations metrics (same as those in Appendix C) and the feature ensemble (Ens.) proposed in Section 2.5. We would like to stress that this study includes training 640 different models and evaluating each model using 6 different metrics.

We can take a few important notes:

- For all examined situations, the proposed normalization always brings a noticeable improvement. The highest improvement is for SimCLR in the presence of pollution; this is consistent with our analysis in the main text.
- For different datasets, different algorithms, and different pollution ratios, the proposed ensembling has the best performance most of the time, and the second best otherwise, which shows how generic our proposed ensembling scheme is.
- k-Cos (Mah) is the metric most often getting second best results among all evaluated, and as such was chosen for our simple baseline (ensemble-free comparison).
- Although in many times it is not the best or second best metric, c-Cos is the metric that gets the largest boost in performance after applying normalization, which is expected because as the ID representation gets more compact, the center is much more representative of the distribution.

H BACKGROUND AND RELATED WORK

H.1 ANOMALY AND OOD DETECTION

Outlier detection is important in a variety of practical tasks, such as detecting problems in a production process, detecting security events, and acting upon novelties. The most general case is unsupervised novelty detection (or poisoned data): there are outliers in the training set, and we have no information about them. Then there are degrees of supervision, semi-supervised (a few outliers are labeled) and fully supervised (all outliers are labeled). Furthermore, in the sub-field of anomaly detection it is assumed that there are no outliers in the training data. A challenge in OOD detection is that the notion of in- and out-of-distribution is not well defined, and task-dependent. A good OOD method would generalize to different notions of out-of-distribution and datasets, e.g. with respect to color, style, perspective and content. Recent approaches in Anomaly/OOD detection can be categorized in four groups:

- **Density-based methods** are based on the assumption that models trained to fit the in-distribution data will be less confident on out-of-distribution data in terms of likelihood of the outputs. Using the likelihood as a detection score has been shown to be a weak metric (Nalisnick et al., 2018; Choi et al., 2018), and modifications such as entropy, energy (Du & Mordatch, 2019; Grathwohl et al., 2019) and WAIC (Choi et al., 2018) have been proposed.
- **One-class classifiers** are a classic approach for outlier detection and have been adopted to deep learning settings. They find a decision boundary that separates ID and OOD samples. A margin is introduced to allow generalization (Schölkopf et al., 2000; Ruff et al., 2018).
- **Reconstruction-based methods** model the ID training data by training an encoder and decoder network to reconstruct the in-distribution data. The reconstruction will generalize less for OOD data such that the reconstruction loss can be used as the detection metric. Auto-encoders (Zong et al., 2018; Pidhorskyi et al., 2018) and GANs (Schlegl et al., 2017; Deecke et al., 2018; Perera et al., 2019).
- **Self-supervised methods** leverage the representations learned from self-supervision, combined with different detection scores. The current state-of-the-art in OOD detection is CSI

Table 11: Detailed ablation study. Here **p** is the ratio of outlier data inside the training set. **Norm** is whether normalization is applied or not. **Ens.** is our proposed feature ensembling. Best results are in **bold**. Second best results are underlined.

Data	Algo	p	Norm	k-Cos	k-Cos (MAH)	c-Cos	c-Cos (MAH)	GDE	Ens.
C10	BYOL	0	✗	84.9	<u>88.5</u>	51.3	83.8	86.2	88.9
		0	✓	89.9	<u>90.5</u>	79.5	89.0	89.5	91.9
		0.1	✗	62.7	<u>82.9</u>	63.4	82.0	80.5	85.3
		0.1	✓	77.5	<u>85.3</u>	78.5	83.6	83.0	88.3
	SimSiam	0	✗	86.5	<u>89.5</u>	59.3	85.8	87.9	90.1
		0	✓	91.6	<u>91.7</u>	84.9	90.5	91.0	92.5
		0.1	✗	65.8	<u>83.2</u>	67.9	81.5	80.7	84.3
		0.1	✓	80.6	<u>86.3</u>	82.5	84.9	84.3	88.4
	SimCLR	0	✗	79.3	<u>86.3</u>	45.6	84.9	84.7	87.8
		0	✓	86.0	<u>88.9</u>	75.2	87.9	88.0	90.3
		0.1	✗	53.1	<u>65.6</u>	62.6	<u>65.9</u>	64.7	80.3
		0.1	✓	68.8	<u>79.8</u>	<u>80.0</u>	78.7	78.2	86.7
	SimCLR(-)	0	✗	88.6	<u>90.7</u>	79.1	90.0	90.1	91.1
		0	✓	91.2	<u>92.9</u>	87.3	92.5	92.6	93.0
		0.1	✗	71.4	<u>79.6</u>	83.4	80.8	80.2	86.3
		0.1	✓	77.9	<u>83.9</u>	<u>87.2</u>	83.6	83.1	87.8
C100	BYOL	0	✗	78.6	<u>79.6</u>	49.4	74.8	76.8	81.3
		0	✓	<u>81.0</u>	80.2	59.5	77.5	78.2	83.4
		0.1	✗	74.1	<u>76.2</u>	50.8	71.4	73.4	77.7
		0.1	✓	<u>78.0</u>	77.8	59.5	75.0	75.7	80.7
	SimSiam	0	✗	79.7	<u>81.4</u>	55.6	77.1	78.8	83.3
		0	✓	<u>84.5</u>	84.3	72.1	82.7	83.1	86.6
		0.1	✗	73.1	<u>78.9</u>	54.7	75.4	75.4	79.7
		0.1	✓	79.7	<u>80.3</u>	67.2	78.4	78.4	82.5
	SimCLR	0	✗	76.3	<u>77.0</u>	35.5	76.3	<u>78.2</u>	84.2
		0	✓	80.1	82.0	68.4	82.6	<u>82.7</u>	86.9
		0.1	✗	69.2	<u>75.9</u>	46.5	75.0	73.8	79.9
		0.1	✓	75.8	<u>80.0</u>	65.6	79.2	78.6	83.0
	SimCLR(-)	0	✗	83.4	84.7	68.5	84.9	<u>85.9</u>	87.9
		0	✓	85.8	87.0	80.3	87.4	<u>87.8</u>	89.4
		0.1	✗	78.1	80.5	67.3	<u>81.1</u>	81.0	84.3
		0.1	✓	81.2	82.8	79.5	<u>83.9</u>	83.6	85.8
fMNIST	BYOL	0	✗	90.5	95.3	84.7	95.0	<u>95.4</u>	95.9
		0	✓	93.2	<u>95.1</u>	91.2	94.8	95.0	96.2
		0.1	✗	38.1	61.3	84.9	75.5	75.2	86.7
		0.1	✓	48.0	73.2	<u>86.9</u>	80.9	80.9	87.9
	SimSiam	0	✗	92.7	95.9	84.7	95.7	95.8	<u>95.8</u>
		0	✓	93.9	<u>95.0</u>	90.7	94.8	94.9	96.1
		0.1	✗	40.3	63.0	88.4	73.3	72.6	<u>86.1</u>
		0.1	✓	52.7	75.3	90.3	80.0	79.8	<u>87.8</u>
	SimCLR	0	✗	87.6	94.6	70.4	95.0	<u>95.1</u>	96.1
		0	✓	91.3	94.9	86.8	94.9	<u>95.0</u>	96.3
		0.1	✗	30.9	46.5	88.4	55.5	55.0	<u>86.3</u>
		0.1	✓	34.9	53.1	90.6	61.1	60.6	<u>87.5</u>
	SimCLR(-)	0	✗	92.7	<u>94.7</u>	86.3	94.5	94.5	95.6
		0	✓	94.2	<u>95.7</u>	90.4	95.6	95.6	95.9
		0.1	✗	60.9	<u>78.7</u>	90.5	83.7	83.5	<u>90.4</u>
		0.1	✓	65.3	80.9	92.1	84.4	84.3	<u>90.9</u>

(Tack et al., 2020), using representations learned by SimCLR (Chen et al., 2020a) and the distance to the closest training point in latent space as a detection score. Other approaches train networks with predefined tasks such as permutations of image patches or rotations (Golan & El-Yaniv, 2018; Hendrycks et al., 2019; Bergman & Hoshen, 2020)].

H.2 SELF-SUPERVISED LEARNING (SSL)

SSL is a form of unsupervised learning, tackling it through means of supervised learning from pseudo-labels that can easily be generated. One line of computer vision research uses augmentations as pseudo-labels. These augmentations can be generated at no additional human cost, for example 90 degree rotations results in four labels. In jigsaw tasks (Noroozi & Favaro, 2016) the image is split in grids, for example 2x2 or 3x3, and shuffled, the resulting position is the prediction target.

Another more recent direction is constrastive learning (Oord et al., 2018; He et al., 2019; Misra & van der Maaten, 2019; Grill et al., 2020a). In SimCLR (Chen et al., 2020a;b) every image in a batch is augmented twice, and the objective is to minimize the distance of the latent representations of the same origin image, while maximizing the distance to other images in the batch.

Another recent SSL direction is non-contrastive or positive samples only SSL. Bootstrap Your Own Latent (BYOL) (Grill et al., 2020b) was the first example of this class of algorithms to achieve very competitive results, that even surpasses SimCLR. BYOL gets away from the problem of representation collapse (first enemy of SSL, usually handled by negative samples) by introducing assymetry in the network architecute through the idea of a prediction network after the project head, it also uses an exponential moving average of the weights of the network as a target representation. SimSiam (Chen & He, 2020) made a significant analysis on BYOL and found that using a moving average of the weights wasnot necessary and just a simple `stop-grad` operation was enough.